





Evaluation of Power Maximization and Curtailment Control Methods for Converters in Wearable Photovoltaic Energy Harvesting Applications

F. SELIN BAGCI ¹ (Graduate Student Member, IEEE), KATHERINE A. KIM ¹ (Senior Member, IEEE),
YU-CHEN LIU ² (Senior Member, IEEE), AND YI-HUA LIU ³ (Senior Member, IEEE)

¹Department of Electrical Engineering, National Taiwan University, Taipei 106, Taiwan

²Department of Electrical Engineering, National Taipei University of Technology, Taipei 106, Taiwan

³Department of Electrical Engineering, National Taiwan University of Science and Technology, Taipei 106, Taiwan

CORRESPONDING AUTHOR: KATHERINE A. KIM (e-mail: kakim@ntu.edu.tw)

This work was supported by the National Science and Technology Council of Taiwan under Grant MOST 109-2218-E-002-011-MY3.

ABSTRACT As wearables become more widely adopted, powering them from ambient energy sources can improve reliability and reduce reliance on batteries. Solar photovoltaic (PV) power is a viable power source for such emerging applications. However, because wearable applications bend and move with the user's motion, the PV panels used in these applications experience varying light intensities over multiple PV cells that reduce power generation in traditional series-string configurations. To address the PV power reduction problem, a configuration of boost converters with parallel-connected outputs are utilized, which is effective in uneven lighting conditions. Depending on the load demand and available solar power, a converter control system should quickly transition between maximum power point tracking (MPPT) and power curtailment operation. This work evaluates MPPT (perturb & observe and constant-voltage) algorithms and power curtailment (over-voltage shut-off and flexible power point tracking) methods on their effectiveness in wearable applications. Experimental results verify that the perturb & observe with flexible power point tracking effectively adapts to changes in the load and light conditions while maintaining 30% and 31% higher output power, respectively. It also maintains the maximum component temperature below 29 °C which is a safe temperature for wearable applications.

INDEX TERMS DC-DC converter, energy harvesting, maximum power point tracking (MPPT), power curtailment, solar photovoltaic (PV) systems, wearable applications.

I. INTRODUCTION

Conventionally, photovoltaic (PV) power has been used for stationary applications with uniform lighting because it is well known that uneven lighting and partial shading drastically decrease output power when PV panels are connected in series [1]. However, in applications such as wearable devices, nonuniform lighting and frequent transients are unavoidable. Wearable sensors and devices can be used for biomedical, health monitoring, or commercial applications [2]–[4], which typically rely solely on batteries that need to be recharged

or replaced. This work focuses on emerging wearable applications that utilize solar PV energy to generate sustainable power [5], [6]; specifically, the converter and controller design considerations to most effectively provide reliable output power.

While PV-powered wearable devices are still emerging applications, their effectiveness has been shown in previous literature. Work in [7] examined the power output of a solar-powered bag using commercial PV cells under realistic outdoor lighting conditions. By measuring solar irradiance

profiles on the PV-powered bag application, it was verified that 2-5 W of power was harvested even under rapidly changing irradiance. Other work in [8] examined a PV-powered backpack able to provide 2-8 W of power, depending on the type of PV cell used. Power levels greater than 0.3 W are generally sufficient to start charging low-power mobile devices. Another aspect of enabling a wider range of wearable PV applications are flexible PV cells. Recent innovations have enabled PV cells to be manufactured on textiles [9], but further development is needed before they are commercially viable. However, PV cells on flexible plastic substrates are currently commercially available.

A. CHALLENGES IN WEARABLE PV DEVICES

Despite offering great potential for capturing ambient solar energy while the device is used, integrating PV panels into wearable devices comes with its own challenges. Unlike more traditional stationary PV applications, the wearability of the device is as important as its technical functionality and a critical factor to consider in the design process. This means the user should be able to use the device comfortably, without discomfort from the structure of the PV panel or circuitry. For this reason, the PV panel selection and placement on the user's body should be given careful consideration. Another design constraint unique for wearable applications is the lower maximum allowable temperature. According to [10], 44 °C is the threshold for human pain from contact burns and 40 °C results in a hot sensation on human skin. Since the wearable may come in contact with skin, the temperature of any component in the device must stay below 40 °C to reduce discomfort and ensure the wearer's safety.

On the other hand, one of the biggest technical challenges is unavoidable mismatch in illuminance across the PV cells which can cause substantial power loss if the system is not properly designed. In larger, rigid PV panels, this loss mainly occurs because of sunlight variation, such as partial shading, across series-connected PV cells. However in wearables, PVs are likely to undergo frequent partial shading (e.g. caused by user motion or the form factor of the garment/body part). Rather than using a long series connection of PV cells that result in a higher voltage, reducing the string length or utilizing a parallel connection of cells improves output power when illumination is not uniform [7]. Additionally, the converter system controlling the PV panels should be able to quickly adjust to rapid changes in incoming light which is expected in wearables due to their non-stationary nature. Similarly, PV power should be reliably delivered to the load, regardless of the load connectivity and its characteristics. In other words, operation should not be affected by different loads being connected or disconnected intermittently as long as the incoming light intensity (even with fluctuations) is sufficiently high.

Since energy harvesting applications have low power budgets, another critical design consideration is the loss in the converter and the power consumption of the microcontroller. To achieve a self-sustaining and highly-reliable system, a lower-power microcontroller employing a control algorithm

with low power consumption is key. Moreover, it is important for the energy harvesting converter system to start automatically once the PV power is sufficient to start charging the load.

B. EXISTING CONTROL ALGORITHMS FOR SOLAR ENERGY HARVESTING

Numerous MPPT techniques have been developed to maximize PV output power and ensure efficient system operation [11]. The majority of traditional MPPT strategies has been geared towards medium- and high-power systems, where the power consumption of the controller is negligible compared to the converter power rating [12]. The main goal of MPPT control is to regulate the PV panel at the MPP, thus, maximizing the generated PV power. Traditional grid-connected PV systems continually run MPPT control because the grid-connection acts as an infinite load that can accept the full amount of PV power generated.

On the other side of the power range, energy harvesting applications have a specific load (i.e., not an infinite load) and the power requirements of the controller are not negligible. In these applications, the MPP does not always correspond to the most favorable operating point of the PV. If the power of the PV panel exceeds the power that the load can accept, overload may occur, such as exceeding the maximum voltage or current rating of the components, resulting in component damage. Therefore, it is imperative to sustain a balance between the generated PV power and the load such that the generated PV power does not exceed the load requirements [13]. To achieve this, power curtailment control algorithms can be utilized to reduce the PV power output to an appropriate level. One type of these control methods, originating from grid-connected PV systems, are flexible power point tracking (FPPT) algorithms, which have been explored as a hybrid control method with MPPT in [14]–[16]. Their purpose is to regulate the PV power to meet a specified power that is lower than the MPP and the specified power can be dynamically changed by a controller.

Further, for successful implementation of MPPT at lower power, the power consumed by the control circuit should be minimal and methods requiring high-level computations and high power consumption should be avoided [17]. There is a trade-off between simplicity in implementation and tracking efficiency, which is particularly pertinent in non-stationary applications, including wearables, that experience fast-changing light conditions [18], [19].

In terms of existing control methods implemented in wearables, a low-power wearable application utilizing both thermal and solar energy harvesting has been discussed in [20], where a commercial chip using a fractional open-circuit voltage (OCV) method was employed. Multiple PV cells were grouped and placed in parallel on separate sections of a jacket in order to ensure similar lighting conditions for each group. While the partition of cells proved useful in reducing the effects of partial shading, the results indicated a maximum efficiency of 67% on a sunny day which was reduced to 48% on a cloudy day. The authors noted the spikes and drops in output power when the user was in motion and mentioned that

a more optimized power control strategy was required to keep up with fast-changing irradiation and to increase the efficiency of the solar wearable.

Another low-power wearable energy harvester was proposed in [21]. Fast and efficient MPPT was achieved by using the output current as the sole control parameter. However, the load was assumed to be fixed during operation which is not the case for all USB-device loads as the voltage characteristics are affected by the power provided to the load [22]. In addition, a flexible bracelet with solar energy harvesting was presented to power biomedical sensors in [23]. A fractional OCV MPPT was implemented with a commercially-available ultra low-power energy harvester. Harvested power charged up a small lithium battery which then powered the sensors. The efficiencies were recorded to reach 85-90%, but the MPPT IC did not have any thermal protection mechanism for temperatures below 85 °C. For wearable applications, this temperature limit is too high and would cause contact burns on human skin and might also be dangerous with a battery in very close proximity.

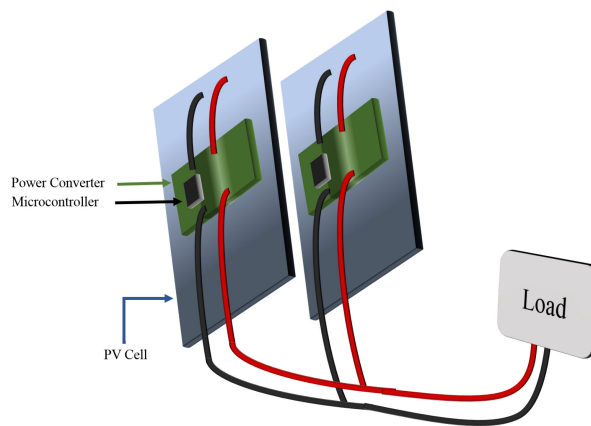
C. TARGET PV-POWERED WEARABLE APPLICATION

The target application is a wearable PV bag system, supplying up to 2.4 W, with a nominal output voltage of 5 V based on USB specifications. The target load is a mobile device with a rechargeable battery, charged through a standard USB connector, such as a mobile phone or a portable battery pack. The initial converter implementation of the target application was realized with single-ended primary-inductor converters (SEPICs) used in a parallel differential power processing (DPP) architecture [24], which was chosen to mitigate the effects of nonuniform light intensities over the panels. The dc-dc converters were placed in between the dc bus and their adjacent PV panel to offset the voltage differences between each panel and the common bus [25]. Using this DPP implementation, a 14.9% improvement was observed from the standalone SEPIC efficiency to the overall system efficiency, but the maximum system efficiency remained below 80%. In the current implementation, it was determined that a direct converter topology (without galvanic isolation) would yield higher system efficiency at the target power level of a few watts, so a standard boost converter topology is utilized.

Fig. 1(a) shows the PV-powered bag prototype with flexible PV panels attached to the bag's surface and a USB cable connected to a mobile phone load. Fig. 1(b) shows the proposed power system structure with the converter mounted behind the PV panels and then connected together. When the bag is in use, the PV panels attached to the fabric will point at different angles and receive different irradiance levels [22]. However, the conventional method of connecting all cells in series does not effectively transfer PV power to the load [7]. Voltage characteristics of PV cells tend to be less sensitive to extreme light differences, therefore parallel configuration proves to be more advantageous when severe mismatch is expected [26]. Unlike traditional rigid PV panels, flexible PV panels exhibit a wider range of maximum power point (MPP)



(a)



(b)

FIGURE 1. PV-powered wearable bag (a) prototype and (b) power system structure.

voltage attributed to the degree of bending they experience when in use [27]. Therefore, individual maximum power point tracking (MPPT) of each panel is advantageous to maximize power.

This work evaluates various power converter system control methods for their effectiveness in low-power wearable devices, where uneven lighting conditions are expected over multiple PV panels. Specifically, an effective control should maximize the PV power transferred to the load when it can accept the full PV power, curtail PV power when the load cannot accept the full power, and transition quickly between the two operation modes. Based on this evaluation, the most appropriate combination of MPPT and curtailment control methods are implemented in a PV-powered wearable system used to charge mobile devices. The contributions of this work are: 1) outlining the specific challenges of power converters used in wearable applications and the need for both MPPT and power curtailment control, 2) performance evaluation of the constant-voltage and perturb-and-observe-based

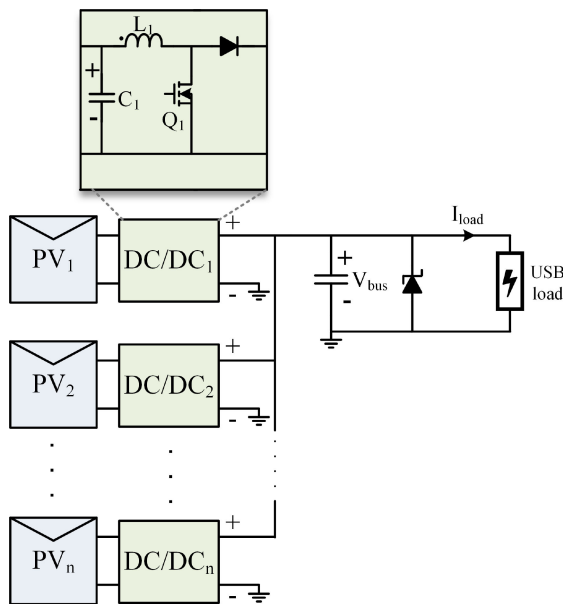


FIGURE 2. System diagram of parallel-connected boost converters.

MPPT algorithms, as well as over-voltage turn-off and active power curtailment, 3) experimental validation of the perturb-and-observe-based MPPT with power curtailment control implemented on multiple parallel boost converters connected in parallel. The control method is implemented on a low-cost microcontroller and its performance is validated through experimentation using 1-W boost converter prototypes. The final control strategy quickly and smoothly transitions from MPPT to power curtailment control according to the changing load conditions.

II. CONVERTER ARCHITECTURE

The converter architecture for the wearable device consists of multiple boost converters whose outputs are connected in parallel to a common bus, as shown in Fig. 2. The bus is then connected to the load, which is a mobile USB device that nominally operates at 5 V. The PV panel specifications should be selected such that the PV panel MPP voltage is lower than the dc bus voltage. If the PV MPP voltage becomes higher than the bus voltage, exact MPPT cannot be maintained. Although the nominal output voltage is 5 V, the dc bus voltage can decrease below 4 V when charging battery loads [22]. Thus, the MPP voltage of the selected PV panels should be less than the minimum expected dc bus voltage.

Because of the diode in the boost converter topology, the system starts up automatically when PV power is produced. Once light hits the PV panel, it produces current that flows through the inductor and the diode to charge the bus capacitor. When the bus voltage is high enough to turn on the microcontroller, the control algorithm starts, which begins switching operation of the converter. Self-startup is essential for energy harvesting applications, like wearables, especially in this type of design that does not include a battery.

The diode of the converter also serves to block continuous reverse current. This ensures that load power does not dissipate through the PV panel when there is no direct irradiance. Since the irradiance levels on the PV panels in this application are expected to vary widely, reverse current flow protection is a requirement.

III. SYSTEM CONTROL ALGORITHMS

A major challenge of PV energy harvesting applications is that the potential input PV power may be at or above the range of power that the load can accept. Moreover, in wearable devices, the input power can transition quickly and frequently between the different levels of power relative to the load power. For this reason, the system control algorithm should quickly transition between these states and maximize power to the load while ensuring the temperature is within a safe range.

A. EXISTING ENERGY HARVESTING IC ALGORITHMS

The existing control algorithms used in integrated circuits (ICs) for energy harvesting applications function under varying PV power levels but do not necessarily have smooth transitions nor ensure maximum power transfer to the load in all situations. For example, the BQ24650 [28] manufactured by Texas Instruments is a low power harvester battery management IC for a buck converter, suitable for PV solar applications. When in MPPT mode, it implements the constant-voltage method, where the PV voltage is regulated to a fixed reference by adjusting the battery charge current. The reference value is usually chosen as the rated MPP voltage from the datasheet of the PV. Additionally, the fractional OCV method is also a common MPPT method used by commercial energy harvesting ICs, such as the BQ25504 [29] also manufactured by Texas Instruments. However, since in this application, the load voltage can be lower than the OCV of the PV panels, the PV voltage would clamp to the output voltage when the OCV is read by the IC, resulting in an incorrect OCV measurement. For this reason, fractional OCV MPPT is not appropriate and only the constant-voltage method is considered for this application.

Both of these harvesting ICs employ the same power management strategy where the converter is operated in MPPT mode until the output voltage exceeds a preset overvoltage value, over which the converter turns off completely and no power is transferred from the PV to the load. Hysteresis is added such that the converter (executing MPPT) will turn on again once the output voltage falls below a lower voltage threshold. In other words, if the potential PV power is higher than the load power, the PV will transition between MPPT and turning off, such that the average provided power does not result in overload. While this control scheme avoids overload and, in turn, excessive heat, it is not necessarily the most effective for maximizing power to wearable applications. This is because turning the converter on and off leads to slow reaction times, particularly, when the input or load powers fluctuate as expected in wearable applications. Moreover, among the MPPT algorithms, neither the fractional OCV

nor the constant-voltage algorithm consistently have a high tracking efficiency which results in unnecessary power loss when optimal output power is desired.

For this reason, alternate control schemes must be explored to consistently maximize PV power in the various conditions that wearable devices experience. In this paper, constant-voltage MPPT in conjunction with over-voltage shut-off control is considered as the conventional energy harvesting method and will be referred to as such. Additionally, its performance will be compared to the proposed control algorithm outlined in the following section.

B. PROPOSED SYSTEM CONTROL METHOD

For PV wearable systems, the load will either be able to accept the maximum available PV power or it will not (i.e. transferring all available PV power would cause overload). When the system switches between these two conditions, the controller should transition between them while protecting against output power interruption, overload, and over heating. With these considerations in mind, a control scheme is proposed for PV wearable devices to improve the output power reliability compared to existing commercial solutions.

1) MAXIMUM POWER POINT TRACKING

When the load is able to accept the full power, the produced PV power should be maximized using an MPPT algorithm to optimize the power produced by the PV panel. This work utilizes the standard P&O MPPT algorithm [30] to continually track the MPP of the PV panel. Since the load can accept the full output power, the bus voltage will be maintained within the acceptable USB voltage range. USB-device loads are nominally 5 V, but their voltage can range from approximately 3 V to 5.2 V depending on the output power and load characteristics [22]. During operation, the bus voltage depends on the impedance of the load and the supplied power, such that the bus voltage is not regulated to a specific voltage but settles to an equilibrium point based on the source-load power balance. If the PV power becomes too low such that it is not sufficient to charge the load, the bus voltage will remain low until the PV power increases to a high enough power to raise the bus voltage and begin charging the load again. If only one PV panel has low power, the diode of the converter prevents power from the dc bus from flowing backwards into the PV panel, preventing additional power loss.

2) POWER CURTAILMENT

If the load is disconnected or PV power increases significantly, maximum PV power will become higher than the power that the load can accept. If this occurs and the PV power is not curtailed, the power imbalance will cause the bus voltage to increase. For over-voltage protection, a zener diode is connected in parallel over the load. The zener breakdown voltage is 5.6 V which prevents the output voltage from overvoltageing and damaging the USB load. The power rating of the zener diode should be at or above the combined nominal power of

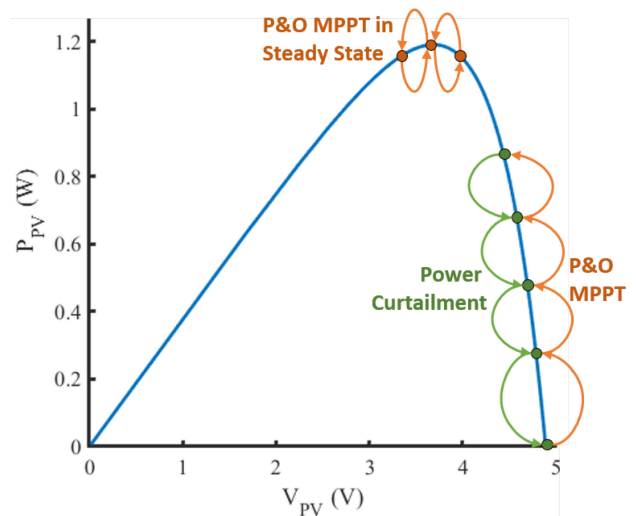


FIGURE 3. PV power curve showing MPPT and curtailment operating points.

the PV panels to avoid overcurrent of the component; in this work the power rating was 3 W. However, if the PV power is not curtailed, the excess energy will dissipate through the zener diode, which raises the temperature of the component. For user safety and comfort, the generated PV power should be curtailed to match the load power.

As opposed to the commercial control algorithm that completely turns off the converter, we propose that a power curtailment method should be used for wearable PV applications. Fig. 3 shows the proposed power curtailment algorithm, which increments the PV voltage until the PV power decreases enough to match the load power. This type of algorithm was previously proposed in [31], [32], intended for larger-power grid-connected PV systems. The algorithm can easily be implemented in tandem with P&O and automatically adapt to either low-power load or no-load conditions. When there is no load, the algorithm increments the PV voltage (thereby, lowering the power) until it reaches the OCV and the converter stops switching. When there is a low-power load, the algorithm increments the PV voltage until the PV power starts to fall below the load power; which results in the bus voltage eventually decreasing below a set threshold voltage such that the control mode returns to MPPT to increase the power again. In light load conditions, the control will alternate between MPPT mode and curtailment mode such that the average power matches the load. Between the MPPT and curtailment modes, the threshold voltage of the bus voltage is changed to add hysteresis in the control algorithm. Because the curtailment control gradually reduces power rather than abruptly turning the converter off and on, the response to changes in input or output power are smoother and maintain more consistent power to the load.

3) OVERALL CONTROL METHOD

The flowchart for the control algorithm is shown in Fig. 4. The controller is initialized in P&O MPPT mode and the threshold

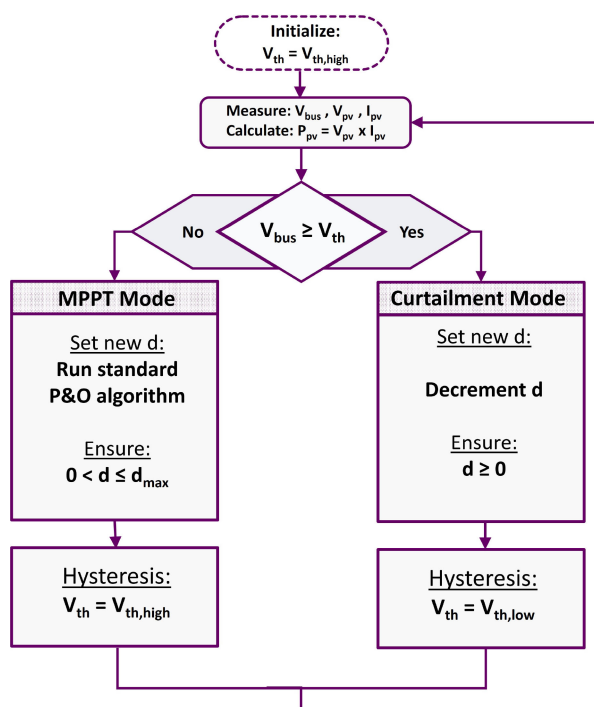


FIGURE 4. System control flowchart.

voltage V_{ih} is set to the higher threshold voltage $V_{ih,high}$, which is typically above 5.1 V in implementation. The controller measures the bus voltage, PV voltage, and PV current. If the bus voltage is lower than V_{ih} , PV power is calculated and the controller runs the P&O MPPT algorithm that changes the converter duty ratio. In this implementation, the converter duty ratio is increased or decreased by an increment of 1.8% during each perturbation cycle. If the bus voltage increases higher than V_{ih} , the control goes into curtailment mode such that the converter duty ratio is decremented, increasing the PV voltage as shown in Fig. 3; then, V_{ih} is set to the lower threshold voltage $V_{ih,low}$, which is around 4.6 V in implementation. After a short delay, the controller measures the bus voltage, PV voltage, and PV current to begin the cycle again. Another way to think about the algorithm is as a state machine with two states: MPPT and curtailment, where the transition into each state occurs when the bus voltage goes below or above the threshold voltage, respectively.

Each boost converter is independently controlled by a Texas Instruments MSP430F5529 microcontroller to control the operation of its associated PV panel. There is a voltage sensor for the bus voltage, a voltage sensor for the PV voltage, and a current sensor for the PV current. The current sensor utilizes a shunt resistor and a differential amplifier to measure the current through the PV panel. The microcontroller and gate driver are powered from the bus, so the controller turns on once the dc bus voltage is above 3.3 V and continues to operate as long as the bus voltage is sufficiently high.

The MSP430 is an ultra-low power controller which can be programmed to achieve low power consumption and is

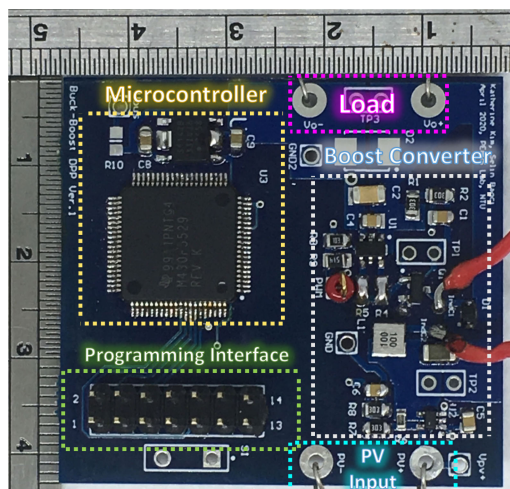


FIGURE 5. Wearable application boost converter hardware.

generally low cost. It was operated with a clock frequency of 12 MHz such that 1.8% was the smallest possible duty ratio increment. A smaller duty ratio increment (resulting in higher tracking effectiveness) could be achieved if the clock frequency is increased, but the controller will also consume more power. In this implementation, it was found that a clock frequency of 12 MHz struck a balance between MPPT effectiveness and controller power consumption. However, these parameters could be adjusted for applications with higher or lower PV power levels.

The proposed MPPT and curtailment algorithm uses established algorithms originating from grid-connected PV systems and adapts their operation for implementation in lower-power wearable applications. The intent is to strike a balance between performance and low power consumption. The next section compares the performance of the proposed control method with existing energy harvesting control methods through experimental results.

IV. EXPERIMENTAL RESULTS

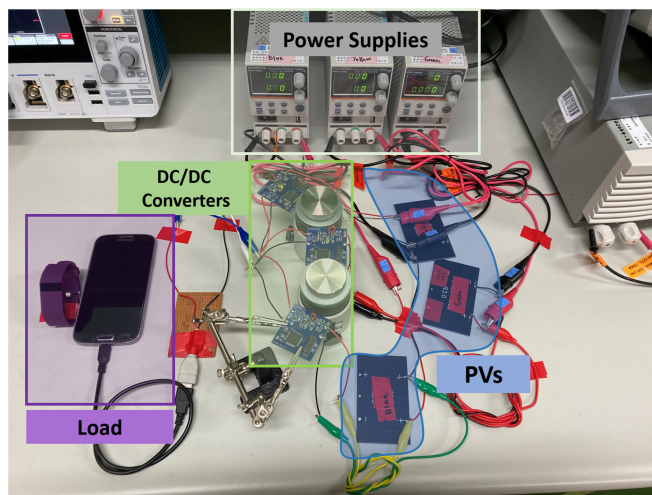
A. EXPERIMENTAL PROTOTYPE AND SETUP

The boost converter was designed and implemented on a printed circuit board (PCB) that includes the Texas Instruments MSP430F5529 microcontroller, with JTAG interface for programming the microcontroller. Both the proposed and conventional control methods were programmed onto the same microcontroller to directly compare the effect of the control method on the output performance. The PCB is shown in Fig. 5 and is less than 4.5 cm by 4.5 cm in area. The converter specifications and parameters are outlined in Table 1. The converter was designed to operate in discontinuous conduction mode (DCM) up to the full output power and utilizes a small, commercially-available inductor.

The hardware system was tested indoors using a controllable PV emulation technique, where a power supply acting as a current source emulates the PV photocurrent and the power

TABLE I Boost Converter Parameters

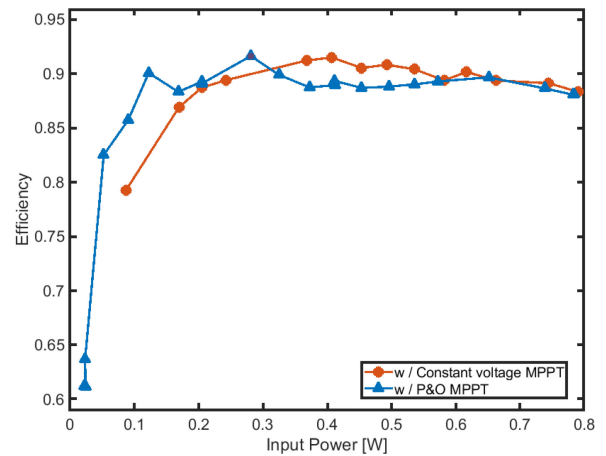
Specification/Component	Value
Switching Frequency	200 kHz
Conduction Mode	DCM
Inductance	10 μ H
Inductor	Würth Elektronik 74438336100
Input Voltage	4.0 V (nominal)
Input Current	0.25 A (maximum)
Output Voltage	5.0 V (nominal)
Output Current	0.2 A (maximum)
Output Power	1.0 W (maximum)
MOSFET	BSS806NH6327
Diode (Schottky)	CUS08F30,H3F
DC Bus Capacitor	220 μ F
Output Capacitor	100 μ F
Gate Driver	ZXGD3000E6
Zener Breakdown Voltage	5.6 V
Microcontroller	TI-MSP430F5529


FIGURE 6. Experimental setup with three PV panels and three converters tested with a mobile phone load.

supply is connected in parallel to a covered PV panel [33]. The PV panels used in the experiment were the IXYS-SM531K08 L with its rated MPP at 4.46 V and 0.218 A. For the load, an electronic load was used in constant voltage mode for some experiments and various USB loads, including a mobile phone and an activity tracker, were used in other experiments. The experimental setup with three power supplies, three PV panels, three converters, and a mobile phone load is shown in Fig. 6.

B. CONTROLLER POWER CONSUMPTION

In the target wearable application, the system must be self-powered from the low-power PV panel. Thus, the power consumption of the microcontroller running the control algorithm is determined by measuring the input power of the system when the microcontroller is both externally-powered and self-powered from the PV panel at the same output power. The power lost to the microcontroller is equivalent to the difference in input power at the same output power level between the two systems. The average power consumption was


FIGURE 7. Measured system efficiency over the power range using P&O vs. constant-voltage MPPT.

measured while the controller was operating in MPPT for the conventional controller (constant-voltage control) and the proposed controller (P&O), which were 2.4 mW and 0.95 mW, respectively. The controller with the constant-voltage algorithm draws 2.5 times more power than it does with the P&O algorithm. We attribute this difference to the use of the PI controller in implementing the constant-voltage control, while the P&O algorithm was implemented without using one. Although, one additional sensor than the constant-voltage algorithm was employed for the implementation of P&O algorithm, the overall power consumption is lower. For a 1-W converter, the controller power consumption is approximately 0.2% or lower of the total power.

C. SYSTEM EFFICIENCY

To evaluate the performance of the PV system under different control methods, both the ability to track the MPP of each PV along with converter and auxiliary losses should be considered. Here, the term system efficiency that captures both of these aspects is defined as

$$\eta_{sys} = \frac{P_{load}}{\sum_{k=1}^n P_{MPP,k}} \quad (1)$$

where P_{load} is the power of the load, n is the number of PV panels, and $P_{MPP,k}$ is the maximum power of PV_k ($k = 1, 2, \dots, n$).

To measure the performance of one PV panel and boost converter, the system efficiency was measured experimentally for the conventional and proposed control methods. The experimental results are shown in Fig. 7 over the input power range. Note that efficiency measurements include the power consumed by the controller, gate driver, and sensors. Measurements were taken while the MPPT algorithm was running: constant-voltage for the conventional method and P&O for the proposed control method.

As shown on Fig. 7, when the P&O algorithm is used, operation starts up around 0.02 W with 62% efficiency. With the conventional constant-voltage algorithm, the converter is

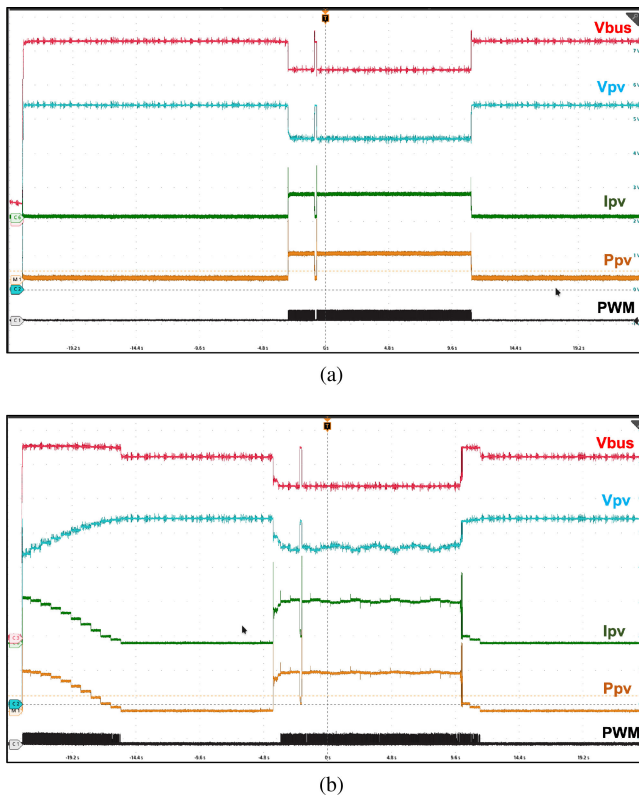


FIGURE 8. Experimental waveforms for when the load was connected to and disconnected from a single-PV system using the (a) conventional and (b) proposed control algorithm.

only able to operate above 0.1 W of input power with a minimum efficiency of 79%. At the same power level of 0.1 W, the efficiency with P&O algorithm reaches 85%, while the maximum efficiency over the operating range is 91%. Using the constant-voltage algorithm, a maximum system efficiency of 92% is achieved (at 407 mW of input power). These measurements are taken assuming rated conditions of the PV panel, such that the MPP voltage is approximately equal to the reference value of the constant-voltage algorithm, resulting in high efficiency above 0.35 W. At non-rated conditions, the efficiency of the constant-voltage MPPT is expected to be lower. Overall, the P&O MPPT algorithm shows consistently high efficiency over a wider operating range than the constant-voltage algorithm.

D. SINGLE CONVERTER AND SINGLE PV PANEL

The converter system is first tested with one boost converter and one PV panel. Three different conditions, all of which are expected to occur during use, were tested using the conventional and proposed control methods: 1) connecting a load, 2) disconnecting a load, and 3) sudden irradiance changes. Fig. 8 shows how both algorithms react to connecting and disconnecting a load, where the waveforms represent the bus voltage (pink), PV current (green), PV voltage (blue), PV

power (orange) and the gate-source voltage of the MOSFET (black).

First, the conventional energy harvesting method is tested using a smartphone as the load. In Fig. 8(a), initially, there is no load connected and the converter is immediately turned off since the bus voltage exceeds the threshold. After the load is connected, the algorithm reacts in 10 ms and reaches the rated MPP in 0.16 s. PV power stays steady during this interval because constant-voltage MPPT is employed. When the load is disconnected, the bus voltage increases above the threshold and MPPT operation stops. The converter reacts in 6.6 ms and it takes 0.12 s for it to completely halt switching.

Next, the experiment is repeated using the proposed control method with the same load and the waveforms are shown in Fig. 8(b). Similarly, there is no load connected during start-up and the controller is in curtailment mode because the bus voltage is above the threshold. As the PV voltage is increased in increments, PV power gradually decreases until it reaches 0 and the converter stops switching. When the load is connected, it starts drawing power from the voltage bus, which decreases the output voltage. When output bus voltage goes below the threshold, the control algorithm goes into MPPT mode. The algorithm reacts to this change in load conditions in 2 ms. The MPP of the PV panel is reached after 0.57 s, as shown by the repeating three-step pattern of the PV voltage. The PV power immediately increases to a level that can charge the load when the load is first connected, then steadily increases as the MPP is reached. When the load is disconnected again, causing the output bus voltage to increase over the threshold voltage, the controller goes back into curtailment mode. The PV voltage is incremented until the PV power reaches 0, and switching is halted. The initial reaction takes 8.82 ms, while the converter is turned off completely after 1.012 seconds.

These experimental results verify that both algorithms transition between MPPT and curtailment modes successfully when a load is connected or disconnected. The proposed algorithm is observed to react 5 times faster to connecting of a load, while it takes approximately 3.6 times longer to settle at MPP. The average power values recorded during the constant-voltage and P&O MPPT are 556.6 mW and 572 mW, respectively. Note that the real MPP voltage is still quite close to the rated value, which is used as the reference in constant-voltage algorithm, at this power range. Even so, the P&O algorithm outperforms the constant-voltage algorithm. When the load is taken away, the switch is gradually turned off as opposed to instantly shutting off. As a result, it takes almost 10 times longer for the proposed algorithm to turn the converter completely off. However, this is not necessarily a downside, as the proposed method allows for smoother transitions that maintain a steadier output power.

Next, Fig. 9 shows the operation with an activity tracker as the load, which is a much lighter load than the smartphone, for both the conventional (over-voltage shut-off) and proposed (flexible power point tracking) curtailment methods. The load can take full P_{mpp} at the beginning, so both algorithms start off

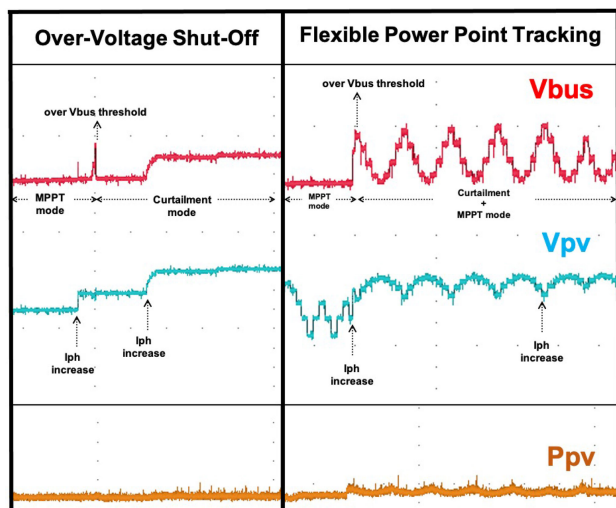


FIGURE 9. Experimental waveforms for when a light load is used.

in MPPT mode. A slight increase in emulated photocurrent, thus P_{mpp} , causes both bus voltages to go over the threshold. The over-voltage shut-off curtailment method turns off the converter instantly and the bus voltage is decreased below the threshold. On the other hand, the flexible power point tracking curtailment method decreases the bus voltage in steps until an acceptable power level is reached. In this case, the bus voltage steps down until it hits the lower threshold voltage. As a result, MPPT mode is triggered which causes the bus voltage to step up until the higher threshold voltage is reached. The algorithm continues to alternate between MPPT and curtailment modes without completely turning off the converter. The bus voltage continually steps between V_{mpp} and V_{oc} such that the average bus voltage is kept below the threshold. Notice that the voltage waveforms have a similar pattern to when MPP is reached with P&O MPPT. More power is transferred to the load with the flexible power point tracking curtailment method as observed in Fig. 9.

In order to examine how the system reacts to sudden irradiance changes, another experiment was conducted using the same setup with a single PV panel and a single boost converter. The lighting changes were replicated by adjusting the photocurrent from the power supply over approximately 2 minutes, as shown in Fig. 10(a). Two digital multimeters logged the input and output power continuously, while an activity tracker was used as the load. The experiment was conducted using the conventional algorithm first, and the proposed algorithm directly after. Then, the same procedure was repeated in reverse order to ensure the results are not affected by the state of charge (SOC) of the load. The averages of the PV and load power are shown in Fig. 10(b). Rather than the power produced by the PVs following the emulated photocurrent (shown in Fig. 10(a)), the PV power in both control methods closely follow the load power, meaning that the source-load power balance is maintained during operation.

The experimental waveforms for the conventional and proposed algorithms during the same experiment are shown in

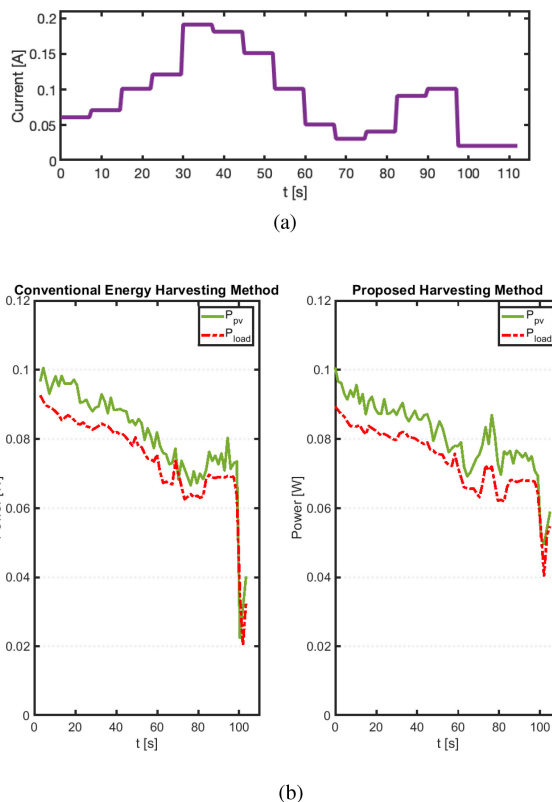


FIGURE 10. (a) The emulated photocurrent and (b) corresponding source-load power with conventional energy harvesting and proposed control method over 120 s.

Fig. 11(a) and Fig. 11(b), respectively. For the majority of the test, the load is not able to accept the maximum PV power, so both algorithms keep the converter switch off until P_{mpp} is low enough to be accepted by the load. Around 70 seconds (labeled as 1), the maximum PV power enters the range of power that can be accepted by the load such that both algorithms initiate MPPT.

However, as shown in Fig. 11(a), the bus voltage exceeds the higher bus voltage threshold when in MPPT, and then goes directly below the lower threshold due to the over-voltage mode, such that the bus voltage oscillates quickly within the hysteresis region. As a result, the PV voltage also oscillates in the same way, which prevents the system from maintaining steady power to the load. In contrast, during the same interval in Fig. 11(b), the algorithm moves between MPPT and power curtailment but in steady increments, such that the PV voltage and resulting output power remain relatively steady. Once the photocurrent is increased at the end of interval 1, both algorithms stop switching.

Then, the photocurrent becomes its lowest (0.01 A) starting from 97 s (labeled as 2), at which point full PV power at MPP can be accepted by the load. Thus, to maximize the generated power, both algorithms initiate MPPT mode. However, MPPT operation can no longer be sustained with the conventional algorithm due to the reference voltage of constant-voltage MPPT being too high for this power range. Additionally, the

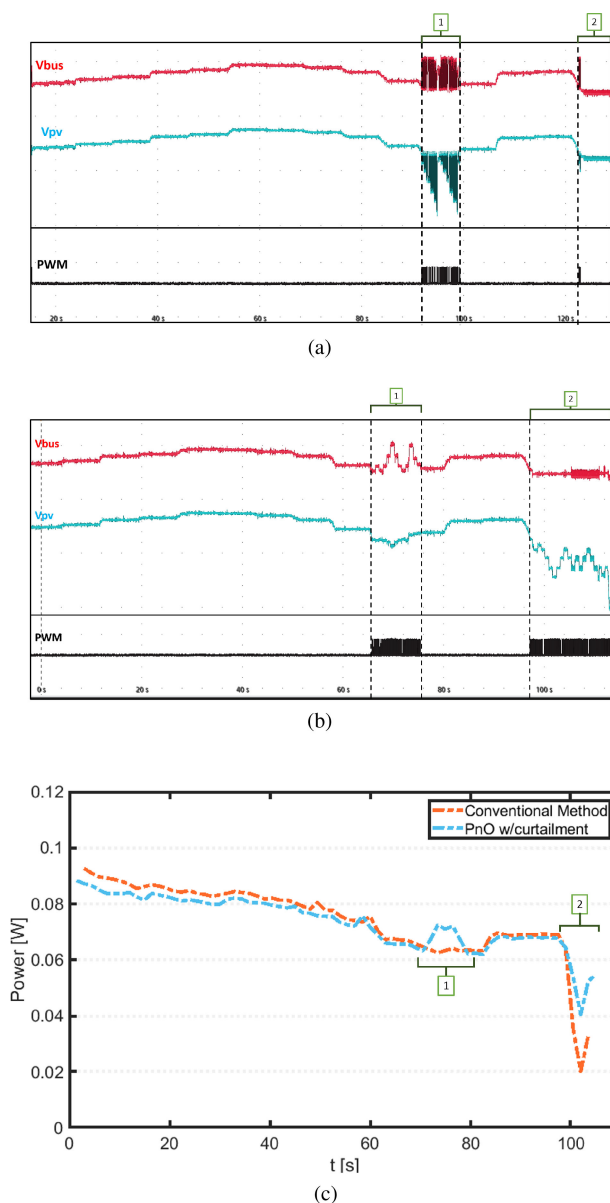


FIGURE 11. Experimental waveforms over 120 s for (a) conventional energy harvesting algorithm and (b) proposed algorithm under dynamic light conditions, and (c) comparison of resulting load powers of the two algorithms.

load is observed to have stopped charging at this point. On the other hand, the proposed algorithm is able to track the real MPP and provide sufficient power to keep the load charging as intended. Comparison of the power provided to the load using each algorithm is shown in Fig. 11(c), where intervals 1 and 2 are labeled. The load power is practically the same when the switch is off. During interval 1, the average power transferred to the load using the conventional and proposed methods were 63.2 mW and 70.6 mW, respectively. During the interval 2, the average power delivered to the load using the conventional method was 29.4 mW, which was not enough to continue charging without interruption. On the other hand,

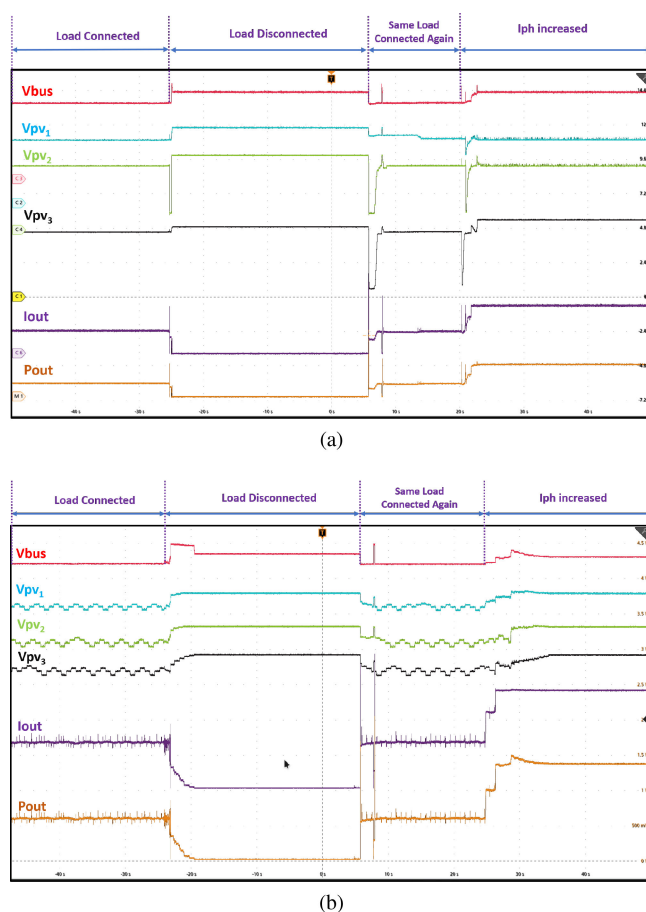


FIGURE 12. Experimental waveforms for a three-panel three-converter system with different PV photocurrents using the (a) conventional and (b) proposed algorithm.

50.3 mW was transferred to the load using the proposed algorithm, which was an improvement of 71%.

E. THREE CONVERTERS AND THREE PV PANELS

Next, an experiment with three boost converters and three PV panels was conducted to investigate the system’s operation with multiple converters under several irradiance and load conditions for both the conventional and proposed control methods. The initial emulated photocurrents for panel 1, 2, and 3 were 0.09 A, 0.03 A, and 0.07 A, respectively. Experimental waveforms representing the bus voltage (pink), each PV voltage (blue, green and black), the output current (purple), and the output power (orange) are shown in Fig. 12. A smartphone was used as the load for both tests which were started after the load had been connected for a few seconds.

The waveforms for the conventional energy harvesting method are shown in Fig. 12(a). Initially, all converters operated in MPPT mode since the bus voltage was lower than the threshold voltage. When all converters were in MPPT mode, the average power drawn by the load was 581.2 mW. After the load was disconnected, bus voltage decreased down below the threshold within 0.18 s. The first two converters effectively

went into curtailment mode by turning their switches off, however the third converter was still switching with a low duty cycle such that it was unable to reach its OCV. Then, the same load was connected again. The second and third PV panels reached the chosen constant MPP voltage in 3 s, while the first one took 8.2 s to find the MPP. The bus voltage adapted to the change in load within 40 ms. The average power transferred to the load during this transition was 443.7 mW. Next, the photocurrent of each PV was increased by 0.10 A, consecutively, from the first to third; that is, emulated photocurrents for panel 1, 2, and 3 became 0.19 A, 0.13 A, and 0.17 A, respectively. After this adjustment, the first and second converters continued in MPPT mode; whereas the third converter responded by turning off, because the increase in photocurrent caused the bus voltage to rise above the threshold. This brief rise in bus voltage did not last long enough to be detected by the first and second converters, hence, they remained in MPPT mode. During this transition, an average of 1.016 W was transferred to the load.

Similarly, the experimental waveforms for the proposed method are shown in Fig. 12(b). Since the load was connected at first, the bus voltage was below the threshold and all converters were in MPPT mode; this was the same as the conventional method. However, the average power transferred to the load during this period was 602.1 mW, approximately 3.6% higher than the conventional method due to different MPPT strategies. After the load was disconnected, it took 3.5 s for the bus voltage to settle below the threshold. The converters did not turn off simultaneously which extended the settling time of V_{bus} compared to the conventional method. Out of the three converters, the second converter turned off last since its panel had the lowest photocurrent, thus, it took the longest to reach its OCV. When the same load was connected again, the bus voltage was brought down below the threshold in 40 ms, same as the conventional method. However, MPP was reached within 3 s. During this transition, 575.8 mW was provided to the load, which was a 29.7% improvement compared to the conventional method during the same transition. After the photocurrent of each PV was increased, all converters went into curtailment mode. Throughout the photocurrent adjustment, the average power transferred to the load was 1.333 W which is 31% higher than the conventional method.

F. MAXIMUM TEMPERATURE

The main objective of implementing the curtailment mode of the control algorithm is to prevent excessive temperature in any other component of the converter. The temperature limit for a wearable device that touches the skin is 40 °C to ensure user safety. Therefore, temperature of the zener diode, which is the hottest component, was measured from startup with no load. A thermal couple was placed on the zener diode while the ambient temperature was approximately 25 °C.

The PV panel and converter system was tested under three control methods: 1) without curtailment (MPPT only), 2) the proposed control method (MPPT and curtailment), and

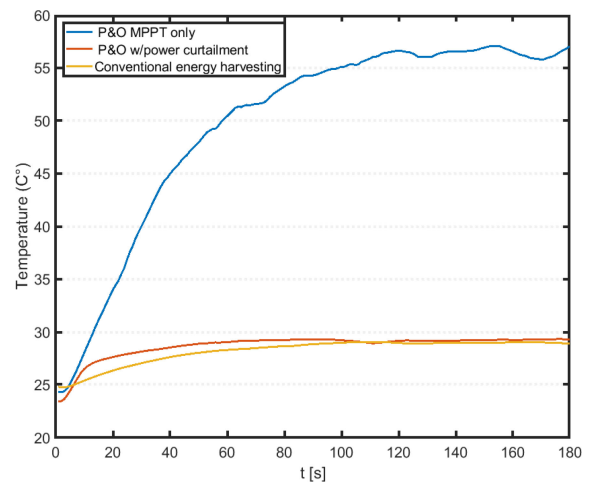


FIGURE 13. Zener diode temperature during start-up using no power curtailment, the conventional energy harvesting algorithm, and the proposed algorithm.

3) the conventional energy harvesting control method. Measured temperature results for these three tests are shown in Fig. 13. The temperature for the algorithm without power curtailment reached 57 °C during the measurement window and continued to rise, which is well above the temperature limit of 40 °C. This emphasizes the need for a power curtailment algorithm to maintain a safe temperature. Conversely, the temperature settled to around 28 °C with both curtailment methods, while peaking at 29.3 °C and 29.0 °C with the proposed and conventional control methods, respectively. While the peak values were similar, the proposed curtailment method initially demonstrated a faster increase in temperature (evident from the steeper curve seen in Fig. 13) because the converter takes some time to turn off, as opposed to turning off instantly when the bus voltage threshold is exceeded. These results verified that both algorithms were successful at keeping the temperature at a safe level for users. The proposed algorithm is just as effective as the conventional algorithm at limiting the temperature despite maintaining a steadier output power.

V. DISCUSSION

The proposed converter control method has been applied to a specific wearable bag application, but the system design is intended to be scalable such that more PV panels and converters can directly be connected to one common load bus. Note that with this design, the PV element connected to each converter can be a single panel or multiple panels in parallel. With multiple PV panels in parallel, each PV may not operate at its exact MPP. If the parallel panels receive similar amounts of light and bend in a similar fashion, their MPP voltages will be similar and the MPPT algorithm will still be effective. However, if the parallel panels are placed in such a way that one receives little or no light, it may sink power from the other panels connected in parallel; in this case, one PV panel per converter is the more effective system architecture.

The converter design in this work has one controller per converter and the controllers are independent. This means that there is no synchronization between converters, however if the controllers are powered on at the same time, the timing of their clocks may be similar. When three converters were tested, excessive ripple interaction (e.g. positive interference) among converters was not observed. However, if a system has many converters that start at the same time, such that combined ripple becomes excessive, a synchronized and interleaved control scheme could also be considered.

For the MPPT algorithm, the standard P&O with a fixed duty ratio step was shown in this work, but other versions of the P&O algorithm may also be effective in wearable applications. Variations such as variable-step P&O may improve tracking effectiveness but it is important to consider if there are additional computational requirements that will cause the microcontroller to consume more power. The balance of these two trade-offs is critical for low-power PV applications.

The goal in this project was to make a scalable converter solution that could be applied to any wearable system with many low-power PV panels that receive different amounts of light or are bent at different angles. Future work will focus on further miniaturization and integration of the converter solution. Control solutions that reduce the required number of sensors may also be explored to further reduce size and cost. Ultimately, utilizing flexible printed circuit boards will be explored with the goal of seamless integration into wearable applications.

VI. CONCLUSION

Solar power is a viable energy source for many emerging wearable applications which tend to experience varying light intensities over the PV cells. Individual MPPT of each PV is essential under such nonuniform light conditions in order to optimize the power output. However, in low-power wearable applications, sustaining the balance between the generated PV power and the load demand is just as important. This work compared and evaluated a conventional energy harvesting control method with the proposed control method that transitions smoothly between MPPT and power curtailment modes while matching the available PV power and load demand of the system. PV power is curtailed by changing the operating point when the load demand is low, whereas the operation proceeds at MPP when the load can accept the full PV input power. Both control methods were compared through experimentation using a wearable PV system that powers USB devices at 5 V.

Experimental results demonstrated that each dc-dc converter successfully controlled its PV panel at the MPP and supplied maximum power to the USB device load when the load was able to accept the full power. Results also showed that the control algorithm properly transitioned from P&O MPPT to power curtailment mode, maintaining source-load balance. Moreover, it was demonstrated that the proposed algorithm reacted to the connecting of a load 5 times faster than the conventional energy harvesting algorithm. Additionally,

it was shown that the proposed algorithm provided higher load power than the conventional algorithm by 29.7% when a load was connected and 31% when the input power was increased. At input power levels below 0.1 W, the proposed control algorithm delivered 71% more power to the load. The load also charged with a steadier output power with the proposed algorithm, while the charging operation was occasionally interrupted with the conventional energy harvesting method under the same conditions. Ultimately, experimental measurements indicate that the proposed control method performed better than the conventional method in terms of reaction time to changes in source or load power, power provided during transients and at lower input power levels, and steady output power distribution. The parallel converter system and the control algorithm provided continuous power to a range of USB loads, even when irradiance conditions changed dynamically. Also, user safety was ensured by the power curtailment algorithm which limited the maximum temperature of the converter below 29 °C.

Although wearable applications are still an emerging technology, the power converter system control solution validated in this work addresses the specific challenge of optimizing power from multiple PV panels that receive different amounts of light while maintaining load-source power balance. Addressing these challenges in the power converter is a step towards making PV-powered wearables more viable. These control solutions also enable PV panels to be utilized as a renewable energy source for other types of mobile PV application, such as drones, electric vehicles, and emergency power equipment.

REFERENCES

- [1] T. Shimizu, M. Hirakata, T. Kamezawa, and H. Watanabe, "Generation control circuit for photovoltaic modules," *IEEE Trans. Power Electron.*, vol. 16, no. 3, pp. 293–300, May 2001.
- [2] A. Pantelopoulou and N. G. Bourbakis, "A survey on wearable sensor-based systems for health monitoring and prognosis," *IEEE Trans. Syst., Man, Cybern., Part C. (Appl. Rev.)*, vol. 40, no. 1, pp. 1–12, Jan. 2010.
- [3] J. Roh, Y. Chi, J. Lee, Y. Tak, S. Nam, and T. J. Kang, "Embroidered wearable multiresonant folded dipole antenna for FM reception," *IEEE Antennas Wireless Propag. Lett.*, vol. 9, pp. 803–806, 2010.
- [4] S. C. Mukhopadhyay, "Wearable sensors for human activity monitoring: A review," *IEEE Sensors J.*, vol. 15, no. 3, pp. 1321–1330, Mar. 2015.
- [5] T. V. Tran and W. Chung, "High-efficient energy harvester with flexible solar panel for a wearable sensor device," *IEEE Sensors J.*, vol. 16, no. 24, pp. 9021–9028, Dec. 2016.
- [6] K. Yu, S. Rich, S. Lee, K. Fukuda, T. Yokota, and T. Someya, "Organic photovoltaics: Toward self-powered wearable electronics," *Proc. IEEE*, vol. 107, no. 10, pp. 2137–2154, Oct. 2019.
- [7] F. S. Bagci, K. A. Kim, T.-Y. Lin, and Y.-C. Liu, "Power profile measurement and system design analysis for a wearable photovoltaic application," in *Proc. IEEE Int. Power Electron. Motion Control Conf.*, 2020, pp. 1469–1474.
- [8] O. Veligorskyi, M. Khomenko, R. Chakirov, and Y. Vagapov, "Performance analysis of a wearable photovoltaic system," in *Proc. IEEE Int. Conf. Ind. Electron. Sustain. Energy Syst.*, 2018, pp. 376–381.
- [9] J. Liu, Y. Li, M. Li, S. Arumugam, and S. P. Beeby, "Processing of printed dye sensitized solar cells on woven textiles," *IEEE J. Photovolt.*, vol. 9, no. 4, pp. 1020–1024, Jul. 2019.
- [10] *Standard Guide for Heated Syst. Surf. Conditions that Produce Contact Burn Injuries*, American Society for Testing and Materials, West Conshohocken, PA, USA, ASTM C1055-03, 2014.

- [11] M. Kordestani, A. Mirzaee, A. A. Safavi, and M. Saif, "Maximum power point tracker (MPPT) for photovoltaic power systems—a systematic literature review," in *Proc. Eur. Control Conf.*, 2018, pp. 40–45.
- [12] T. Eswam and P. L. Chapman, "Comparison of photovoltaic array maximum power point tracking techniques," *IEEE Trans. Energy Convers.*, vol. 22, no. 2, pp. 439–449, Jun. 2007.
- [13] H. D. Tafti et al., "Extended functionalities of photovoltaic systems with flexible power point tracking: Recent advances," *IEEE Trans. Power Electron.*, vol. 35, no. 9, pp. 9342–9356, Sep. 2020.
- [14] Y. Yang, H. Wang, F. Blaabjerg, and T. Kerekes, "A hybrid power control concept for PV inverters with reduced thermal loading," *IEEE Trans. Power Electron.*, vol. 29, no. 12, pp. 6271–6275, Dec. 2014.
- [15] H. D. Tafti, A. I. Maswood, G. Konstantinou, J. Pou, and F. Blaabjerg, "A general constant power generation algorithm for photovoltaic systems," *IEEE Trans. Power Electron.*, vol. 33, no. 5, pp. 4088–4101, May 2018.
- [16] H. D. Tafti, A. Sangwongwanich, Y. Yang, J. Pou, G. Konstantinou, and F. Blaabjerg, "An adaptive control scheme for flexible power point tracking in photovoltaic systems," *IEEE Trans. Power Electron.*, vol. 34, no. 6, pp. 5451–5463, Jun. 2019.
- [17] O. Lopez-Lapena, M. T. Penella, and M. Gasulla, "A new MPPT method for low-power solar energy harvesting," *IEEE Trans. Ind. Electron.*, vol. 57, no. 9, pp. 3129–3138, Sep. 2010.
- [18] K. K. Kumar, R. Bhaskar, and H. Koti, "Implementation of MPPT algorithm for solar photovoltaic cell by comparing short-circuit method and incremental conductance method," *Procedia Technol.*, vol. 12, pp. 705–715, 2014. [Online]. Available: <https://www.sciencedirect.com/science/article/pii/S221201731300738X>
- [19] J. Ahmad, "A fractional open circuit voltage based maximum power point tracker for photovoltaic arrays," in *Proc. 2nd Int. Conf. Softw. Technol. Eng.*, 2010, vol. 1, pp. V1247–V1250.
- [20] Q. Brogan, T. O'Connor, and D. S. Ha, "Solar and thermal energy harvesting with a wearable jacket," in *Proc. IEEE Int. Symp. Circuits Syst.*, 2014, pp. 1412–1415.
- [21] T. Wu, M. S. Arefin, D. Shmilovitz, J.-M. Redoute, and M. R. Yuce, "A flexible and wearable energy harvester with an efficient and fast-converging analog MPPT," in *Proc. IEEE Biomed. Circuits Syst. Conf.*, 2016, pp. 336–339.
- [22] H. Lee and K. A. Kim, "Design considerations for parallel differential power processing converters in a photovoltaic-powered wearable application," *Energies*, vol. 11, no. 12, pp. 1–17, Nov. 2018.
- [23] P. Jokic and M. Magno, "Powering smart wearable systems with flexible solar energy harvesting," in *Proc. IEEE Int. Symp. Circuits Syst.*, 2017, pp. 1–4.
- [24] F. S. Bagci, Y. Liu, and K. A. Kim, "Low-power photovoltaic energy harvesting with parallel differential power processing using a sepic," in *Proc. IEEE Appl. Power Electron. Conf. Expo.*, 2019, pp. 2008–2014.
- [25] H. Jeong, H. Lee, Y. Liu, and K. A. Kim, "Review of differential power processing converters techniques for photovoltaic applications," *IEEE Trans. Energy Convers.*, vol. 34, no. 1, pp. 351–360, Mar. 2019.
- [26] H. Lee and K. A. Kim, "Comparison of photovoltaic converter configurations for wearable applications," in *Proc. Workshop Control Model. Power Electron.*, 2015, pp. 1–6.
- [27] J. Park, H. Joshi, H. G. Lee, S. Kiaei, and U. Y. Ogras, "Flexible PV-cell modeling for energy harvesting in wearable IoT applications," *ACM Trans. Embed. Comput. Syst.*, vol. 16, no. 5s, Sep. 2017, Art. no. 156. [Online]. Available: <https://doi.org/10.1145/3126568>
- [28] "Bq24650 stand-alone synchronous buck battery charge controller for solar power with maximum power point tracking datasheet," Texas Instrum., Dallas, Texas, USA, Tech. Rep. SLUSA75B, Jan. 2020.
- [29] "Bq25504-ultra low power boost converter with battery management for energy harvester applications," Texas Instrum., Dallas, Texas, USA, Tech. Rep. SLUSAH0F, Oct. 2019.
- [30] T. Eswam, J. Kimball, P. Krein, P. Chapman, and P. Midya, "Dynamic maximum power point tracking of photovoltaic arrays using ripple correlation control," *IEEE Trans. Power Electron.*, vol. 21, no. 5, pp. 1282–1291, Sep. 2006.
- [31] A. Sangwongwanich, Y. Yang, F. Blaabjerg, and D. Sera, "Delta power control strategy for multistring grid-connected PV inverters," *IEEE Trans. Ind. Appl.*, vol. 53, no. 4, pp. 3862–3870, Jul./Aug. 2017.
- [32] A. Sangwongwanich, Y. Yang, F. Blaabjerg, and H. Wang, "Benchmarking of constant power generation strategies for single-phase grid-connected photovoltaic systems," *IEEE Trans. Ind. Appl.*, vol. 54, no. 1, pp. 447–457, Jan./Feb. 2018.
- [33] S. Qin, K. A. Kim, and R. C. N. Pilawa-Podgurski, "Laboratory emulation of a photovoltaic module for controllable insolation and realistic dynamic performance," in *Proc. IEEE Power Energy Conf. Illinois*, 2013, pp. 23–29.



ment and control for photovoltaic energy harvesting applications.



Since 2019, she has been an Associate Professor of electrical engineering with National Taiwan University, Taipei, Taiwan. Her research interests include power electronics and control for solar photovoltaic applications.

Dr. Kim was the recipient of the Award for Achievements in Power Electronics Education from the IEEE Power Electronics Society in 2022, recognition as an Innovator Under 35 for the Asia Pacific Region by the MIT Technology Review in 2020, and the Richard M. Bass Outstanding Young Power Electronics Engineer Award from PELS in 2019. Since 2017, she was an Associate Editor for the IEEE TRANSACTIONS ON POWER ELECTRONICS. For IEEE Power Electronics Society, she was the Student Membership Chair in 2013–2014, PELS Member-At-Large for 2016–2018, PELS Women in Engineering Chair in 2018–2020, and the PELS Constitution and Bylaws Chair in 2021 to 2022.



with the Department of Electrical Engineering, National Ilan University, Yilan, Taiwan. Since 2022, he has been an Associate Professor with the Department of Electrical Engineering, National Taipei University of Technology, Taipei, Taiwan. His research interests include analysis and design of zero-voltage-switching dc-dc converters, power factor correction techniques, redundant sever power supplies, and high efficiency converters.



with the Department of Electrical Engineering, National Ilan University, Yilan, Taiwan. Since 2022, he has been an Associate Professor with the Department of Electrical Engineering, National Taipei University of Technology, Taipei, Taiwan. His research interests include power electronics and battery management.